A Broadband and FSS-Based Transmitarray Antenna for 5G Millimeter-Wave Applications

Mei, Peng; Pedersen, Gert Frølund; Zhang, Shuai

Published in:
I E E E Antennas and Wireless Propagation Letters

DOI (link to publication from Publisher):
10.1109/LAWP.2020.3042295

Creative Commons License
Unspecified

Publication date:
2021

Document Version
Accepted author manuscript, peer reviewed version

A Broadband and FSS-Based Transmitarray Antenna for 5G Millimeter-Wave Applications

Peng Mei, *Student Member, IEEE*, Gert Frølund Pedersen, *Member, IEEE*, and Shuai Zhang, Senior *Member, IEEE*

***Abstract*— This letter describes the design of a broadband and FSS-based transmitarray (TA) antenna for 5G millimeter-wave applications. Two different elements are proposed to avoid the issues of the geometrical parameter resizing of the elements to obtain a 2-bit transmission phase of {-π, -π/2, 0, π/2} to achieve a TA antenna with wideband behaviors. Both of the two proposed elements show low insertion loss of below 1 dB from 24 to 38 GHz. Moreover, the two elements can achieve two sets of discrete transmission phases of {– π, 0} and {-π/2, π/2} without resizing their dimensions, respectively. A TA prototype based on the proposed two elements is designed and fabricated. The measured results agree very well with the simulated ones. The measured 1- and 3-dB gain bandwidth is 28.0-37.5 GHz (29.0 %) and 25.1-39.1 GHz (43.7%), respectively. A peak aperture efficiency of 44.7% at 30 GHz is experimentally obtained with a realized gain of 26.1 dBi.**

***Index Terms* — FSS-based, wideband, transmitarray antenna, polarization-rotating.**

I. INTRODUCTION

High gain and wideband millimeter-wave antennas are potentially good solutions to offer high capacity of 2-7 Gb/s to fulfill the rapid growth of mobile data traffic in point-to-point or backhauling communications [1], [2]. Transmitarray (TA) antennas have attracted many interests due to their unique advantages, such as high gain, low cost, simple feeding technique and so on [3]-[6]. Generally, TA antennas suffer from narrow bandwidths due to the resonant properties of the utilized elements. However, the bandwidth limitations of such resonant elements can be improved by optimizing the element structures as reported in [3], [4], [7], [8]. In [4], the authors proposed an element with five metallic layers to achieve a 1-dB gain bandwidth of 24.27% and a maximum aperture efficiency of 62%. The fabrication and implementation of the TA antenna, however, are complicated.

Recently, several novel methods are introduced to design TA antennas with wideband and low-profile properties [9]-[18]. These methods can generally be divided into two categories. The first one is to use different types of elements to provide the required transmission phases that are either continuous or discrete. Each element is responsible for a certain number of discrete transmission phases [9]-[12] or a very small part of the continuous 2π transmission phase range [13], [14]. Since all transmission phases are not dependent on a single element, the bandwidth or profile of such TA antenna can be improved. In [9], C. Jouanlanne *et al*. proposed two different elements based on receiver-transmitter structures to offer a 3-bit transmission phase by resizing the dimensions of the two elements. The 1- and 3-dB gain bandwidth is 15.4% and 20%, respectively, with an aperture efficiency of 42.7% at 61.5 GHz. The other method is to rely on a single element implemented by polarization-rotating (PR) structures to provide either continuous [15] or discrete transmission phases [16], [17]. The element is typically configured with three metal layers and two substrates. The top and bottom layers are all metallic polarizer grids placed orthogonally, and the middle layer is a metallic structure with PR properties [15]-[17]. One PR element can naturally provide two different transmission phases (with a phase difference of π) by simply rotating the middle metal layer π/2. In [17], the authors presented a PR element with cross-shaped metallic strips tilted π/4 in the middle layer to achieve a 2-bit transmission phase by varying the dimensions of the cross-shaped metallic strips. The corresponding TA antenna was fabricated and measured, revealing a 3-dB gain bandwidth of 24.1%. It should be noticed that the bandwidth the element would be shrunk when its dimensions are varied to achieve two or more transmission phases [9]-[17], leading to lower performance of the corresponding TA antenna.

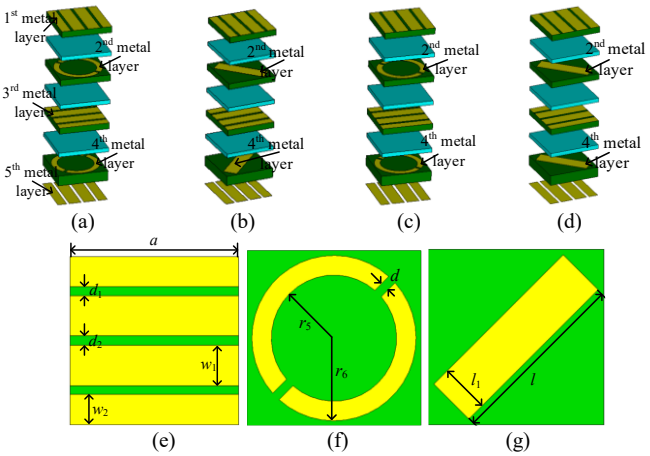

Fig. 1. Geometries of the proposed two FSS-based elements with different

Manuscript received Jan, 2020. This work was supported in part by AAU Young Talent Program and also in part by the InnovationsFonden project of MARS2. (*Corresponding author: Shuai Zhang*)

The authors are all with the Antennas, Propagation and Millimeter-wave Systems (APMS) section, Department of Electronic Systems, Aalborg University, Aalborg, 9220, Denmark. (email: sz@es.aau.dk)

configurations. Expanded view of (a). Element 1 with a "**00**" transmission phase, (b). Element 2 with a "**01**" transmission phase, (c) Element 1 with a "**10**" transmission phase, and (d). Element 2 with a "**11**" transmission phase. Front view of: (e). Polarizer grid of Elements, (f). The 2nd metal layer of Element 1, and (g). The 2nd metal layer of Element 2.

In this letter, we propose a design approach to implement a wideband TA antenna, where two elements with different configurations are proposed to fulfill a 2-bit transmission phase, avoiding resizing the same element. The proposed elements are all based on PR structures with a total thickness of 0.2λ and a unit periodicity of 0.25λ (λ is the wavelength at 30 GHz). Two extra metal layers compared to the PR elements in [15]-[17] are added to make the polarizations of the incident and transmitted waves the same when electromagnetic (EM) wave impinges the element. The proposed two elements are designed to not only provide a 2-bit transmission phase but also maintain low insertion loss in a wide bandwidth. It should be noted that the design approach is also applicable to three-layer elements [e.g. [15]-[17], [19]]. The proposed two elements are described in Section II. The proposed wideband TA antenna is implemented in Section III. Fabrication, measurement, and discussion are carried out in Section IV. Section V concludes the letter finally.

II. Elements Design

As verified and reported in [9]-[11] and [15]-[17], elements that provide 2- or 3-bit transmission phases are sufficiently feasible to implement TA antennas with fairly good performance. The phase quantization losses for TA or RA antennas have been thoroughly investigated in [20]-[22]. In this section, we focus on designing two different elements capable of providing both a 2-bit transmission phase and low insertion loss in a wide bandwidth, without resizing their dimensions.

Fig. 1 presents the geometries of the proposed two elements. Each element consists of five metal layers and four substrate layers. The 1st, 3rd, and 5th metal layers are identical polarizer grids, where the 3rd metal layer is orthogonal to the 1st and 5th metal layers. The 2nd and 4th metal layers are identical polarization-rotating type metallic strips. The supporting substrates (see the green layers in Fig. 1) are Rogers 4003C with a dielectric constant of 3.55 and a loss tangent of 0.0027. The supporting substrate of the 4th metal layer is 0.508 mm thick, while the supporting substrates of the 1st, 2nd, and 3rd metal layers are 0.305 mm thick. Three bonding films (see the blue layers in Fig 1) are employed to glue different Rogers 4003C substrates tightly together. The bonding films used here are Rogers 4450F with a dielectric constant of 3.52, a loss tangent of 0.004, and a thickness of 0.202 mm. The total thickness of the element is 0.2 λ (λ is the wavelength at 30 GHz). The proposed element has the following features compared to the structure with three metal layers described in [15]-[17]:

a). The polarizations of the incident and transmitted waves are the same for the proposed TA antenna by adding the two extra metal layers, while it is orthogonal for the one implemented by three metal layers structure in [15]-[17];

b). The transmission phase of the proposed element is doubled when the EM wave propagates through it since there are two identical polarization-rotating type layers (2nd and 4th metal layer). So, it is much easier to obtain to the required phase than those in [15]-[17], which also helps further broaden the bandwidth.

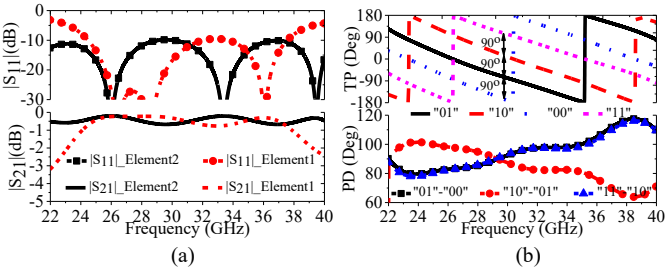

Fig. 2. S-parameters of the proposed two FSS-based elements. (a). Reflection and transmission amplitudes of S_{11} and S_{21}. (b) Transmission phases and phase differences of the two FSS-based elements (TP: transmission phase; PD: phase difference).

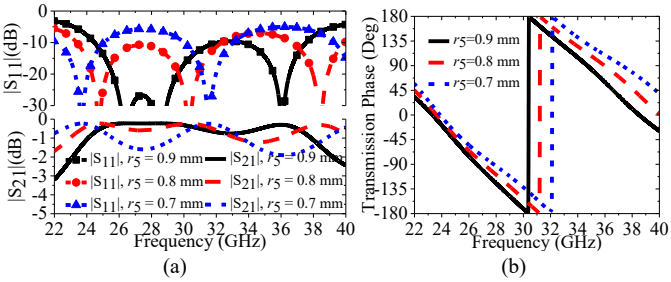

Fig. 3. S-parameters of element 1 with a different value of r_5. (a). Amplitudes of the S-parameters. (b). Transmission phase.

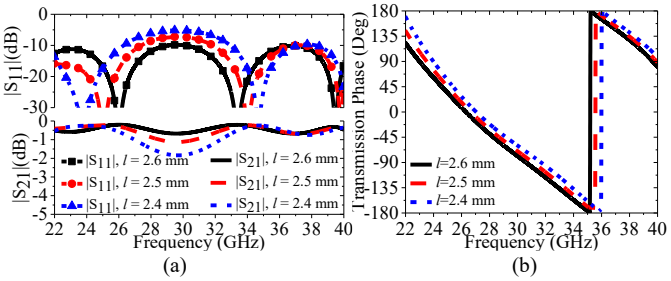

Fig. 4. S-parameters of element 2 with a different value of l. (a). Amplitudes of the S-parameters. (b). Transmission phase.

The expanded views of the proposed two elements are shown in Figs. 1 (a) - (d), where the split circular ring and rectangular metallic strip tilted π/4 are selected as the 2nd and 4th metal layers. The dimensions of the two elements are determined to make them operating in the 5G millimeter-wave bands and given as follows: a = 2.5 mm, d_1 = 0.13 mm, d_2 = 0.14 mm, w_1 = 0.6 mm, w_2 = 0.45 mm, d = 0.13 mm, l = 2.6 mm, l_1 = 0.7 mm, r_5 = 0.9 mm, r_6 = 1.18 mm.

The proposed two elements are polarization-rotating type structures. Each element can naturally provide two transmission phases with a π phase difference by rotating one polarization-rotating metal layer by 90 deg (either 2nd or 4th metal layer in Fig. 1) with all the other dimensions fixed, while still

maintaining the amplitudes of its S-parameters [23],[24]. Here, we fix the 2nd metal layer but rotate the 4th metal layer as shown in Figs. 1 (c) and (d). A 2-bit digital code can be used to characterize the transmission phases of the two elements as seen in Fig. 1, where the element 1 provides the transmission phases of -π and 0, and the element 2 is responsible for the transmission phases of – π/2 and π/2. The S-parameters are carried out with the CST Microwave Studio software. As seen in Fig. 2 (a), the two elements have low insertion loss from 22 to 40 GHz. In particular, the insertion loss is less than 1dB from 24 to 38 GHz for both two elements. The transmission phases of the elements with different codes are given in Fig. 2 (b), where a π/2 transmission phase gradient is achieved from 22 to 40 GHz. The simulated results in Fig. 2 (a) show that the fractional bandwidth with the insertion loss of below 1dB is up to 45.2%, which is much wider than that reported in [9]-[12], [15]-[17]. It indicates that the bandwidth with low insertion loss can be significantly broadened by applying two different elements to provide a 2-bit transmission phase without resizing their dimensions.

Parametric studies are carried out to give some guidelines to control the frequency responses of the two elements. Since the proposed two elements are both the polarization-rotating type structures, the dimensions of the 2nd and 4th metal layers are relatively more sensitive to the frequency responses of the proposed two elements. As seen in Fig. 3 (a), the S-parameter amplitudes of the element 1 vary with r_5 (in Fig. 1 (f)). A bigger r_5 can provide a larger transmission phase delay as shown in Fig. 3 (b). For the element 2, it is observed that in Fig. 4, a bigger l yields better impedance match, smaller attenuation, and a larger transmission phase delay. The desired transmission phases of the proposed two elements can be obtained by optimizing the values of r_5 and l. Besides, the frequency responses of element 1 and 2 can also be manipulated by tuning the values of d and l_1, respectively.

The frequency responses of the proposed two elements under transverse electric (TE) and transverse magnetic (TM) oblique incidence waves are also investigated. Since the unit periodicity of the element is only 0.25λ * 0.25λ (λ is the wavelength at 30 GHz) that can be served as a miniaturized structure, the frequency responses under oblique incidence waves are relatively stable (up to at least π/6), which has been verified by simulations.

III. Wideband Transmitarray Antenna Design

In this section, the proposed two elements with a 2-bit transmission phase are fully employed to construct a TA antenna. A schematic diagram of the TA antenna is shown in Fig. 5 (a). The ratio of F/D is closely associated with the beamwidth of the feeding source and is critical for a TA antenna to achieve a good aperture efficiency. F is the distance from the phase center of the feeding source to the transmit-panel, and D is the size of the transmitarray panel. A linearly polarized horn antenna with a type of "PASTERNACK PE9851/2F-10 is adopted as the feeding source. The dimensions and the radiation patterns of the horn antenna can be found from its datasheet in [25], where the operating frequency ranges from 22 to 33 GHz with a nominal gain of 10.0 dBi. It is feasible to extend its operating frequency up to 40 GHz after comparing the simulated and measured radiation patterns of the horn antenna from 33 to 40 GHz. The polarization of the feeding source is y-polarized as illustrated in Fig. 5(a). Since the proposed TA antenna features with wide bandwidth, the spillover and illumination efficiencies should be considered at different frequencies. After extensive simulations and optimizations, F and D are selected as 70 mm and 85 mm, respectively, leading to an F/D ratio of 0.823. The transmit-panel with the size of 85 mm×85 mm is constructed by 34×34 proposed elements in x- and y-directions. The loss budget of a TA antenna

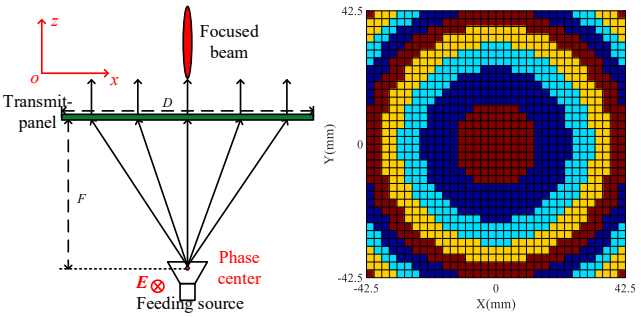

Fig. 5. (a). Schematic diagram of a TA antenna. (b). Phase distributions on the plane of the transmit-panel at 28 GHz.(■: π/2, ■: 0, ■: -π/2, ■: - π.)

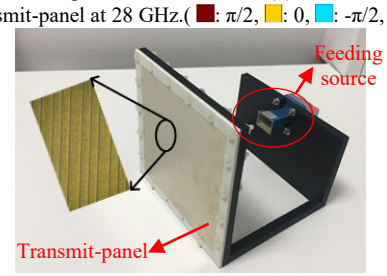

Fig. 6. Photograph of the proposed TA antenna.

Once F and D are determined, the phase distributions on the plane of the transmit-panel are obtained accordingly from the simulations at the frequency of interest, which typically ranges from -π to +π. Since the proposed two elements can only offer four different transmission phases, some approximations should be adopted to make the two elements suitable for a TA antenna design [17]. Using the approximations, the final phase distributions on the plane of the transmit-panel are obtained and plotted in Fig. 5(b). Based on the phase distributions, the transmit-panel is configured with the proposed two elements accordingly, and the full TA antenna is simulated with the CST Microwave Studio. The loss budget of the proposed TA antenna consists of spillover loss, illumination loss, and phase quantization loss, where the spillover and illumination efficiencies are explicitly described in [26].

IV. Fabrication, Measurement, and Discussion

In this section, the proposed TA antenna has been fabricated and measured. The transmitarray panel was produced with a

printed circuit board (PCB) technology [27]. Fig. 6 presents a photograph of the proposed TA antenna. There are 18 air holes with the diameters of 3 mm uniformly distributed at the edge of the fabricated transmit-panel and the 3D printing fixture for assembling them with plastic screws.

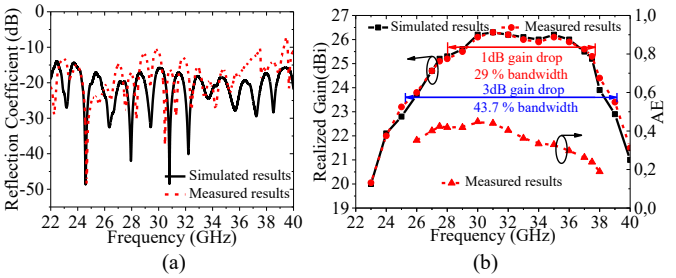

Fig. 7. (a). Measured and simulated reflection coefficients of the proposed TA antenna. (b). Measured and simulated realized gain of the proposed TA antenna and the measured aperture efficiency (AE).

A. Reflection coefficient.

The reflection coefficient of the proposed TA antenna is measured. As seen in Fig. 7(a), the measured -10 dB bandwidth is from 22 to 40 GHz, which aligns with the simulated one. The reflection coefficient at 39 GHz is slightly higher than -10 dB, which is mainly attributed to effects of the coaxial to waveguide transition. In simulation, the coaxial to waveguide transition is not modelled and considered since its specific dimensions are not available from its datasheet.

B. Realized gain and radiation patterns

The realized gain of the proposed TA antenna is measured and presented in Fig. 7(b), where the simulated counterpart is also plotted for comparison. It is observed that the measured results agree very well with the simulated ones. The measured realized gains are slightly higher than the simulated counterparts at some frequencies, which are common in wideband transmitarray antennas [9], [11], [15], [16]. Based on the measured realized gain, the 1- and 3-dB gain bandwidths are calculated, revealing a fractional bandwidth of 29% and 43.7%, respectively. The aperture efficiency is also calculated with the measured realized gain. As seen in Fig. 7(b), the proposed TA antenna can reach a peak aperture efficiency of 44.7% at 30 GHz with the realized gain of 26.1 dBi. The aperture efficiency is above 40.0% from 27 to 32 GHz with a fractional bandwidth of 16.9%.

The radiation patterns of the proposed TA antenna are measured. The normalized radiation patterns at 27.5 and 37.5 GHz are presented in Fig. 8, where the simulated results are also plotted. It is observed that the measured radiation patterns of co-polarization (co-pol) agree with the simulated counterparts. The main beams, first radiation nulls, and sidelobes are consistent between the measured and simulated results as observed from the insets in Fig. 8. Both of the measured sidelobes in E- (*yoz*) and H-plane (*xoz*) at 27. 5 and 37.5 GHz are below -18 dB. The measured normalized cross-polarizations (cro-pol) of the proposed TA antenna are below -30 dB in E- (*yoz*) and H-plane (*xoz*) at 27.5 and 37.5 GHz.

Comprehensive comparisons are made to compare the proposed TA antenna with state-of-the-art TA antennas as summarized and illustrated in Tab. I. It is observed that the proposed TA antenna achieves a wider 1- and 3-dB gain bandwidth and a comparable aperture efficiency by using a 2-bit transmission phase quantization. The thickness of our proposed element is larger than that in [16] and [17] since two extra layers are added to ensure the polarization identical between the feeding source and the entire TA antenna.

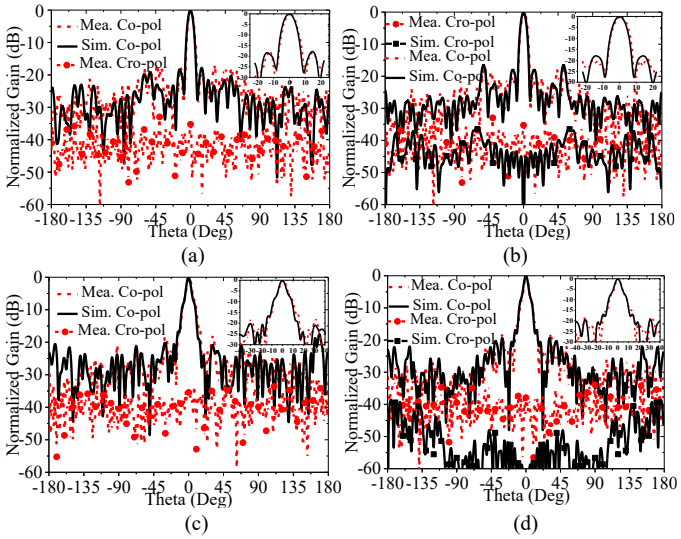

Fig. 8. Measured and simulated normalized radiation patterns of the proposed TA antenna at different frequencies. E-plane (*yoz*) at: (a) 27.5 GHz, (c) 37.5 GHz; H-plane (*xoz*) at: (b) 27.5 GH, (d) 37.5 GHz.

Tab. I. Performance comparison of the proposed TA antenna with other similar TA antennas.

Ref.	f_0/RG (GHz)/ (dBi)	PS /Layers	Thickness	*F/D* Ratio	AE (%)	1/3-dB BW (%)	SG (dBi)
Pro.	**30/ 26.1**	**4/5**	**0.2λ**	**0.82 3**	**44.7**	**29/43.7**	**11.0**
[16]	29/ 25.2	4/3	0.1 λ	0.88	45.2	7*/26.6	14.0
[17]	10/ 27.2	4/3	0.05 λ	1	40.7	16*/24.1	N.A
[9]	61.5/ 32.5	8/3	0.22 λ	0.67	42.7	15.4/20*	14.1

Pro.: Proposed; RG: realized gain; PS: phase states; AE: aperture efficiency; SG: source gain; *: calculated from the measured results; BW: bandwidth.

V. Conclusion

This letter has developed a wideband transmitarray antenna based on FSS-based elements. Two different elements have been utilized to achieve wideband behaviors and avoid the issues of geometrical parameter resizing of the elements to obtain a 2-bit transmission phase. A TA antenna prototype based on the proposed two elements has been fabricated and measured. The measured results agree very well with the simulated ones, revealing a 1- and 3-dB gain bandwidth of 29% and 43.7%, respectively. The prototype reaches a peak aperture efficiency of 44.7% at 30 GHz with a realized gain of 26.1dBi. The proposed TA antenna is a good candidate for 5G millimeter-wave applications due to its wide bandwidth and stable radiation performance.

REFERENCES

[1] T. S. Rappaport *et al*., "Millimeter-wave mobile communications for 5G cellular: it will work!" *IEEE Access,* vol. 1, pp. 335-349, May 2013.

[2] C. Dehos, J. L. Gonzslez, A. De Domenico, D. Ktenas, and L. Dussopt, "Millimeter-wave access and backhauling: The solution to the exponential data traffic increase in 5G mobile communications systems?" *IEEE Commun. Mag.,* vol. 52, no. 9, pp. 88-95, sep. 2014.

[3] A. H. Abdelrahman, A. Z. Elsherbeni, and F. Yang, "High-gain and broadband transmitarray antenna using triple-layer spiral dipole elements," *IEEE Antennas Wireless Propag Lett*., vol. 13, pp. 1288-1291, 2014.

[4] S. Tuloti, P. Rezaei, and F. Hamedani, "High-efficient wideband transmitarray antenna," *IEEE Antennas Wireless Propag Lett*., vol. 17, no. 5, pp. 817-820, May. 2018.

[5] G. Liu, H. Wang, J. Jiang, F. Xue, and M. Yi, "A high-efficiency transmitarray antenna using double split ring slot elements," *IEEE Antennas Wireless Propag Lett*., vol. 14, pp. 1415-1418, 2015.

[6] P. Mei, S. Zhang, X. Q. Lin, and G. F. Pedersen, "A millimeter-wave gain-filtering transmitarray antenna design using a hybrid lens," *IEEE Antennas Wireless Propag Lett*., vol. 18, no. 7, pp. 1362-1365, July 2019.

[7] Y. Cai, W. Li, K. Li, S. Gao, Y. Yin, L. Zhao, and W. Hu, "A novel ultrawideband transmitarray design using tightly coupled dipole elements," *IEEE Trans. Antennas Propag*., vol. 67, no. 1, pp. 242-250, Jan. 2019.

[8] A. Abdelrahman, P. Nayeri, A. Elsherbeni, and F. Yang, "Bandwidth improvement methods of transmitarray antennas," *IEEE Trans. Antennas Propag*., vol. 63, no. 7, pp. 2946-2954, Jul. 2015.

[9] C. Jouanlanne, A. Clemente, M. Huchard, J. Keignart, C. Barbier, T. Nadan, and L. Petit, "Wideband linearly polarized transmitarray antenna for 60 GHz backhauling," *IEEE Trans. Antennas Propag*., vol. 65, no. 3, pp. 1440-1445, Mar. 2017.

[10] A. Moknache, *et al*., "A switched-beam linearly-polarized transmitarray antenna for V-band backhaul applications," the 10th European Conference on Antennas and Propagation (EuCAP), 2011.

[11] F. Manzillo, A. Clemente, and J. Gonzalez-Jimenez, "High-gain D-band transmitarrays in standard PCB technology for beyond-5G communications," *IEEE Trans. Antennas Propag*., vol. 68, no. 1, pp. 587-592, Jan. 2020.

[12] X. Yang, Y. Zhou, L. Xing, and Y. Zhao, "A wideband and low-profile transmitarray antenna using different types of unit-cells" *Micro Opt Technol Lett*., vol. 61, pp. 1584-1589, 2019.

[13] Q. Luo, *et al*., "A hybrid design method for thin-panel transmitarray antennas," *IEEE Trans. Antennas Propag*., vol. 67, no. 10, pp. 6473-6483, Oct. 2019.

[14] X. Yi, T. Su, X. Li, B. Wu, and L. Yang, "A double-layer wideband transmitarray antenna using two degrees of freedom elements around 20 GHz," *IEEE Trans. Antennas Propag*., vol. 67, no. 4, pp. 2798-2802, Apr. 2018.

[15] P. Feng, S. Qu, and S. Yang, "Octave bandwidth transmitarrays with a flat gain," *IEEE Trans. Antennas Propag*., vol. 66, no. 10, pp. 5231-5238, Oct. 2018.

[16] Y. Ge, C. Lin, and Y. Liu, "Broadband folded transmitarray antenna based on an ultrathin transmission polarizer," *IEEE Trans. Antennas Propag*., vol. 66, no. 11, pp. 5974-5981, Aug. 2018.

[17] K. Mavrakakis, H. Luyen, J. Booske, and N. Behdad, "Wideband transmitarrays based on polarization-rotating miniaturized-element frequency selective surfaces," *IEEE Trans. Antennas Propag*., vol. 68, no. 3, pp. 2128-2137, Mar 2020.

[18] N. K. Grady, *et al.*, "Terahertz metamaterials for linear polarization and anomalous refraction," *Science*, vol. 340, no. 6138, pp. 1304-7, Jun 2013.

[19] L. Marnat, K. Medrar, and L. Dussopt, "Highly integrated high gain substrate-integrated planar lens for wide D-band applications," *14th European Conference on Antennas and Propagation (EUCAP)*, 2020.

[20] F. Diaby, *et al*., "Wideband circularly-polarized 3-bit transmitarray antenna in Ka-band," *11th European Conference on Antennas and Propagation (EUCAP)*, 2017.

[21] H. Yang, et al., "A study of phase quantization effects for reconfigurable reflectarray antennas," *IEEE Antennas Wireless Propag Lett*., vol. 16, pp. 302-305, May. 2016.

[22] Robert J. Mailloux, *Phased Array Antenna Handbook*, Third Edition, 2018 Artech House, 685 Canton Street Norwood, MA.

[23] X. Huang H. Yang, D. Zhang, and Y. Luo, "Ultrathin dual-band metasurface polarization converter," *IEEE Trans. Antennas Propag*., vol. 67, no. 7, pp. 4636-4641, Jul. 2019.

[24] X. Gao, X. Han, W. Cao, H. Li, H. Ma, and T. Cui, "Ultrawideband and high-efficiency linear polarization converter based on double V-shaped metasurface," *IEEE Trans. Antennas Propag*., vol. 63, no. 8, pp. 3522-3530, Aug. 2019.

[25] http://everythingrf.com/products/waveguide-horn-antennas/pasternack-enterprises-inc/617-20-pe9851-2f-10

[26] A. Yu, F. Yang, A. Z. Elsherbeni, J. Huang, and Y. Rahmat-Samii, "Aperture efficiency analysis of reflectarray antennas," *Micro Opt Technol Lett*., vol. 52, no. 2, pp. 364-372, Feb 2010.

[27] http://pcbastore.com